 CMES, vol.94, no.1, pp.29-52, 2013

Periodic Collinear Circular-Hole Cracks in an Infinite Plate in Tension

Changqing Miao[1], Yintao Wei[2] and Xiangqiao Yan[1]

Abstract: This paper is concerned with periodic collinear circular-hole cracks in an infinite plate in tension. A numerical approach to this type of circular-hole cracks is presented. Numerical examples are included to illustrate the accuracy of the numerical approach. By means of a generalization of Bueckner's principle and by using a displacement discontinuity method, periodic collinear circular-hole cracks in an infinite plate in tension are investigated in detail by using the numerical approach. Many numerical results are given and discussed.

Keywords: Periodic collinear cracks, Periodic collinear circular-hole cracks, Stress intensity factors, Displacement discontinuity method

1 Introduction

The stress concentration associated with different kinds of geometric discontinuity or notch is important to engineers engaged in the design or life assessment of the tubesheet in nuclear components, such as steam generator, heat exchanger, etc The reliable evaluation for the quantifying the acceptability of local imperfections is of considerable interest to assure the structural integrity of the perforated plate

Collinear periodic cracks are very typical models. Early researchers (e.g., Westergaard (1939), Irwin (1957) and Koiter (1959) studied an infinite row of collinear cracks in an infinite elastic isotropic sheet. Collinear periodic cracks in an anisotropic medium were concerned with by Hu and Zhao (1996) and Cai and Lu(2009). Hu, Huang and Zhong (1997) dealt with collinear periodic cracks in anisotropic bimaterials. Recently, a planar periodic array of collinear cracks at an interface between two dissimilar isotropic materials and periodic interface cracks in piezoelectric materials were investigated by Lekesiz, Katsube, Rokhlin (2011) and Hausler, Gao and Balke(2004), respectively. By using the series expansion variational method, solutions of collinear periodic holes were obtained by Chen and Lin (2007). The other

[1] Res Lab on Composite Materials, Harbin Inst Technol, Harbin, 150001, P.R.China.
[2] Dept Automot Engn, Tsinghua University, Beijing, 100084, P. R China.

related reports also can be seen in Bleuth and Hutchinson (1994), Ouinas (2012), Iovane and Sumbatyan (2009), Wang and Feng (2001), Chen (2011), Hu, Huang and Cheng (1998), Horii, H. and Nemat-Nasser(1985), Nemet-Nasser, Yu, and Hori (1993).

This paper is concerned with periodic collinear circular-hole cracks in an infinite plate in tension, as shown in Fig.1. A numerical approach to this type of circular-hole cracks is presented. Numerical examples are given to illustrate the accuracy of the numerical approach. By means of a generalization of Bueckner's principle and by using a displacement discontinuity method, further, periodic collinear circular-hole cracks in an infinite plate in tension are investigated in detail by using the numerical approach. Many numerical results of the stress intensity factors (SIFs) are given and discussed.

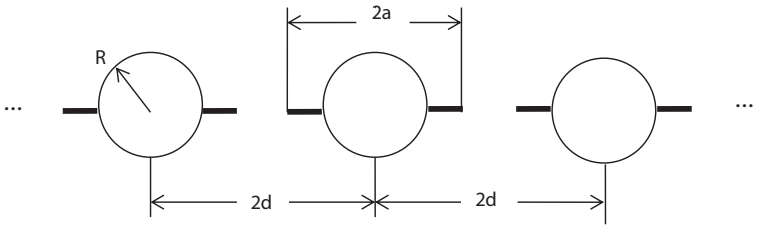

Figure 1: Schematic of periodic collinear circular-hole cracks in an infinite plate

2 A Generalization of Bueckner's Principle

Bueckner (1958) derived an important result, which is related to the principle of superposition. He demonstrated the equivalence of the SIFs resulting from external loading on a body and those resulting from internal tractions on the crack face. The SIFs for a crack in a loaded body may be determined by considering the crack to be in an unloaded body with applied tractions on the crack face only. These face tractions are equal in magnitude but opposite in sign to those evaluated along the line of the crack site in the uncracked configuration.

Recently, Yan (2006a) tried to extend Bueckner's principle suited for a crack to a hole-crack problem in an infinite plate subjected to remote loads, called an original problem for short. The original problem is divided into a homogeneous problem (the one without hole and cracks) subjected to remote loads and a hole-crack problem in an infinite plate in an unloaded body with applied tractions on the crack face and hole face. The applied tractions on the crack face and hole face are equal in

magnitude but opposite in sign to those evaluated along the line of the crack site in the uncracked configuration. Thus, the results in terms of the SIFs can be obtained by considering the latter problem, which is analyzed easily by means of the hybrid displacement discontinuity method proposed recently by Yan (2005*b*).

3 A Numerical Approach to Periodic Collinear Circular-Hole Cracks

In this section, periodic collinear circular-hole cracks in an infinite plate shown in Fig.1 are taken as an example to illustrate the implementation process of the numerical approach.

For periodic collinear circular-hole cracks (called hole-cracks for short) shown in Fig.1, it is possible to label various hole-cracks by numbering from $-\infty, \cdots, -2, -1, 0, 1, 2, \cdots, \infty$, as shown in Fig.2. Thus such as hole-crack (0), hole-crack (2) and hole-crack (-2) can be used to denote hole-cracks 0, 2 and -2 labeled in Fig.2, respectively. Because of periodic collinear symmetry of the hole-cracks, hole-crack (0) can be taken to be investigated and the x and y coordinates system are set up at the center of the geometry center of hole-crack (0), as shown in Fig.3.

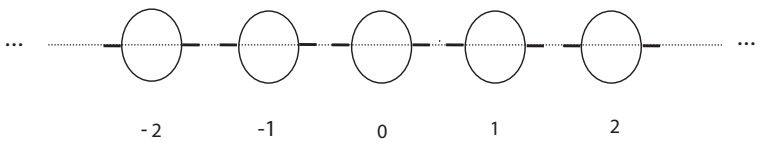

Figure 2: Schematic of numbering of periodic collinear circular-hole cracks

First, the boundary element formulations are carried out for hole-crack (0) by using boundary element methods. Because of the x and y axes symmetries of hole-crack (0), the quadrant of the boundary of hole-crack (0) can be only considered. Thus boundary element discretizations are implemented only for boundary ABC (which is called boundary (0) for short) in Fig.3. It is assumed that N boundary elements with approximately same size are discretized on boundary (0), as shown in Fig.3 in which element 1, element i and element N are labeled. For periodic collinear hole-cracks, an element located at a crack tip is set to be a crack tip displacement discontinuity element. Based on boundary element methods (Crouch and Starfied (1983) and Yan (2005*b*)), the following boundary element formulations can be

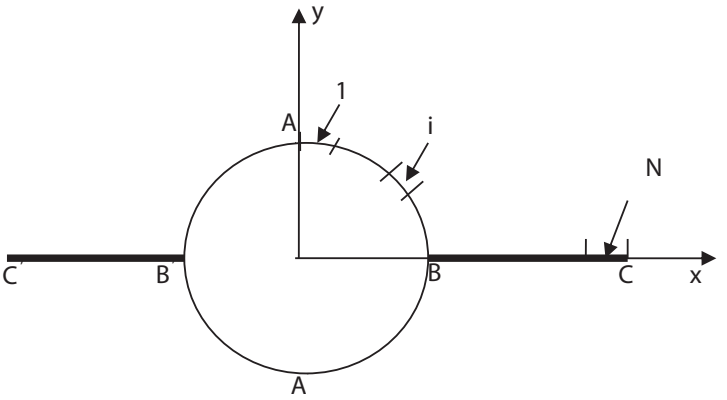

Figure 3: A schematic of hole-crack 0, $x-y$ coordinates and element discretizations (a geometry size and load distribution are not pictured in the figure)

obtained for any element$i$ on boundary (0),

$$\begin{aligned} \sigma_s^{i(0)} &= \sum_{j=1}^{N} A_{ss}^{ij(0)} D_s^j + \sum_{j=1}^{N} A_{sn}^{ij(0)} D_n^j \\ \sigma_n^{i(0)} &= \sum_{j=1}^{N} A_{ns}^{ij(0)} D_s^j + \sum_{j=1}^{N} A_{nn}^{ij(0)} D_n^j \end{aligned} \qquad (i = 1 \text{ to } N) \tag{1}$$

where $\sigma_s^{i(0)}$ and $\sigma_n^{i(0)}$ are the shear and normal stresses on element i on boundary (0) due to boundary (0). $A_{ss}^{ij(0)}$, etc are the influence coefficients of element i on boundary (0) due to element j on boundary (0), which are how to be calculated, to constant displacement discontinuity elements and crack-tip elements, are described respectively by Crouch and Starfied (1983) and Yan (2005b), and $D_s^j$and D_n^j are displacement discontinuities of element j on boundary (0).

Using the symmetries of $x = 0$ and $y = 0$ of hole-crack (0), the effects of element i on boundary (0) due to all boundaries of hole-crack (0) can be considered.

Second, the boundary element formulations are set up for hole-crack (1). Because of the symmetries of $x = 2d$ and $y = 0$ of hole-crack (1), as done for hole-crack (0), the quadrant of the boundary of hole-crack (1) can be only considered and the quadrant boundary of hole-crack (1) is called boundary (1) which corresponds to boundary (0) on the boundary of hole-crack (0). Meantime, boundary element discretizations of boundary (1) are carried out in such a manner that all elements on boundary (1) have the same size as the corresponding elements on boundary (0), as shown in Fig.4. Then the effects of element i on boundary (0) due to the N

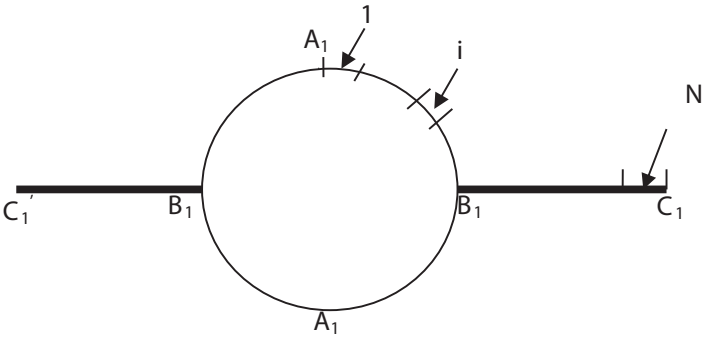

Figure 4: A schematic of hole-crack 1 (or hole-crack -1) and element discretizations

elements on boundary (1) can be expressed as:

$$\begin{aligned}\sigma_s^{i(1)} &= \sum_{j=1}^{N} A_{ss}^{ij(1)} D_s^j + \sum_{j=1}^{N} A_{sn}^{ij(1)} D_n^j \\ \sigma_n^{i(1)} &= \sum_{j=1}^{N} A_{ns}^{ij(1)} D_s^j + \sum_{j=1}^{N} A_{nn}^{ij(1)} D_n^j \end{aligned} \qquad (i = 1 \text{ to } N) \tag{2}$$

where $\sigma_s^{i(1)}$ and $\sigma_n^{i(1)}$ are the shear and normal stresses on element i on boundary (0) due to boundary (1). $A_{ss}^{ij(1)}$, etc are the influence coefficients of element i on boundary (0) due to element j on boundary (1).

Using the symmetries of $x = 2d$ and $y = 0$ of hole-crack (1), the effects of element i on boundary (0) due to all boundaries of hole-crack (1) can be included.

Thirdly, the boundary element formulations are set up for hole-crack (-1). Because of the symmetries of $x = -2d$ and $y = 0$of hole-crack (-1), as done for hole-crack (0), the quadrant of the boundary of hole-crack (-1) can be only considered and the quadrant boundary of hole-crack (-1) is expressed as boundary (-1) which corresponds to boundary (0) on the boundary of hole-crack (0). Boundary (-1) are discretized in such a manner that all elements on boundary (-1) have the same size as the corresponding elements on boundary (0). Thus the effects of element i on boundary (0) due to the N elements on boundary (-1) can be expressed as:

$$\begin{aligned}\sigma_s^{i(-1)} &= \sum_{j=1}^{N} A_{ss}^{ij(-1)} D_s^j + \sum_{j=1}^{N} A_{sn}^{ij(-1)} D_n^j \\ \sigma_n^{i(-1)} &= \sum_{j=1}^{N} A_{ns}^{ij(-1)} D_s^j + \sum_{j=1}^{N} A_{nn}^{ij(-1)} D_n^j \end{aligned} \qquad (i = 1 \text{ to } N) \tag{3}$$

where $\sigma_s^{i(-1)}$ and $\sigma_n^{i(-1)}$ are the shear and normal stresses on element$i$ on boundary

(0) due to boundary (-1). $A_{ss}^{ij(-1)}$, etc are the influence coefficients of element i on boundary (0) due to element $j$on boundary (-1).

Using the symmetries of $x=-2d$ and $y=0$ of hole-crack (-1), the effects of element i on boundary (0) due to all boundaries of hole-crack (-1) can be considered.

For hole-crack (k) and hole-crack $(-k)$, the boundary element formulations can be obtained:

$$\begin{aligned}\sigma_s^{i(k)} &= \sum_{j=1}^{N} A_{ss}^{ij(k)} D_s^j + \sum_{j=1}^{N} A_{sn}^{ij(k)} D_n^j \\ \sigma_n^{i(k)} &= \sum_{j=1}^{N} A_{ns}^{ij(k)} D_s^j + \sum_{j=1}^{N} A_{nn}^{ij(k)} D_n^j\end{aligned} \qquad (i=1 \text{ to } N) \tag{4}$$

and

$$\begin{aligned}\sigma_s^{i(-k)} &= \sum_{j=1}^{N} A_{ss}^{ij(-k)} D_s^j + \sum_{j=1}^{N} A_{sn}^{ij(-k)} D_n^j \\ \sigma_n^{i(-k)} &= \sum_{j=1}^{N} A_{ns}^{ij(-k)} D_s^j + \sum_{j=1}^{N} A_{nn}^{ij(-k)} D_n^j\end{aligned} \qquad (i=1 \text{ to } N) \tag{5}$$

For hole-crack (k), using its symmetries of $x=2k\cdot d$ and $y=0$, the effects of element i on boundary (0) due to all boundaries of hole-crack (k) can be considered.

For hole-crack $(-k)$, using its symmetries of $x=-2k\cdot d$ and $y=0$, the effects of element i on boundary (0) due to all boundaries of hole-crack $(-k)$ can be also considered.

Using the boundary element formulations (1) to (5), we have

$$\begin{aligned}\sum_{m=-k}^{k} \sigma_s^{i(m)} &= \sum_{m=-k}^{k} \Big(\sum_{j=1}^{N} A_{ss}^{ij(m)}\Big) D_s^j + \sum_{m=-k}^{k} \Big(\sum_{j=1}^{N} A_{sn}^{ij(m)}\Big) D_n^j \\ \sum_{m=-k}^{k} \sigma_n^{i(m)} &= \sum_{m=-k}^{k} \Big(\sum_{j=1}^{N} A_{ns}^{ij(m)}\Big) D_s^j + \sum_{m=-k}^{k} \left(\sum_{j=1}^{N} A_{nn}^{ij(m)}\right) D_n^j\end{aligned} \qquad (i=1 \text{ to } N) \tag{6}$$

Based on the superimposition principle, when k in (6) is large enough, the following formulas are right for periodic collinear hole-cracks:

$$\begin{aligned}\sum_{m=-k}^{k} \sigma_s^{i(m)} &= \sigma_s^i \\ \sum_{m=-k}^{2k} \sigma_n^{i(m)} &= \sigma_n^i\end{aligned} \qquad (i=1 \text{ to } N) \tag{7}$$

where σ_s^i and σ_n^i are the average shear and normal load of element i on boundary (0).

From formulas (6) and (7), for periodic collinear hole-cracks, we have

$$\begin{aligned}
&\sum_{m=-k}^{k}(\sum_{j=1}^{N}A_{ss}^{ij(m)})D_s^j+\sum_{m=-k}^{k}(\sum_{j=1}^{N}A_{sn}^{ij(m)})D_n^j=\sigma_s^i\\
&\sum_{m=-k}^{k}(\sum_{j=1}^{N}A_{ns}^{ij(m)})D_s^j+\sum_{m=-k}^{k}\left(\sum_{j=1}^{N}A_{nn}^{ij(m)}\right)D_n^j=\sigma_n^i
\end{aligned}\qquad (i=1\text{ to }N) \tag{8}$$

4 Brief Description of the Hybrid Displacement Discontinuity Method

In this section, the hybrid displacement discontinuity method presented by Yan (2005*b*) is described briefly. It consists of the constant displacement discontinuity element presented by Crouch and Starfield (1983) and the crack-tip displacement discontinuity elements.

4.1 Constant Displacement Discontinuity Element

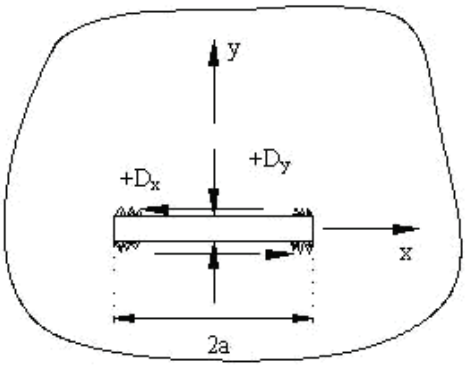

Figure 5: Schematic of constant displacement discontinuity components D_x and D_y

The displacement discontinuity D_i is defined as the difference in displacement between the two sides of the segment (see Fig.5):

$$\begin{aligned}
D_x&=u_x(x,0_-)-u_x(x,0_+)\\
D_y&=u_y(x,0_-)-u_y(x,0_+)
\end{aligned} \tag{9}$$

The solution to the subject problem is given by Crouch and Starfield (1983). The displacements and stresses can be written as

$$\begin{aligned}
u_x&=D_x[2(1-\nu)F_3(x,y)-yF_5(x,y)]+D_y[-(1-2\nu)F_2(x,y)-yF_4(x,y)],\\
u_y&=D_x[(1-2\nu)F_2(x,y)-yF_4(x,y)]+D_y[2(1-\nu)F_3(x,y)-yF_5(x,y)],
\end{aligned} \tag{10}$$

and

$$\begin{aligned}
\sigma_{xx} &= 2GD_x[2F_4(x,y)+yF_6(x,y)]+2GD_y[-F_5(x,y)+yF_7(x,y)],\\
\sigma_{yy} &= 2GD_x[-yF_6(x,y)]+2GD_y[-F_5(x,y)-yF_7(x,y)],\\
\sigma_{xy} &= 2GD_x[-F_5(x,y)+yF_7(x,y)]+2GD_y[-yF_6(x,y)].
\end{aligned} \tag{11}$$

G and $v$in these equations are shear modulus and Poisson's ratio, respectively. Functions F_2 through F_7 are described by Crouch and Starfield (1983). Eqs (2) and (3) are used by Crouch and Starfield (1983) to set up a constant displacement discontinuity method.

4.2 Crack-Tip Displacement Discontinuity Elements

By using the Eqs (10) and (11), recently, Yan (2005*b*) presented crack-tip displacement discontinuity elements, which can be classified as the left and the right crack-tip displacement discontinuity elements to deal with crack problems in general plane elasticity. The following gives basic formulas of the left crack-tip displacement discontinuity element.

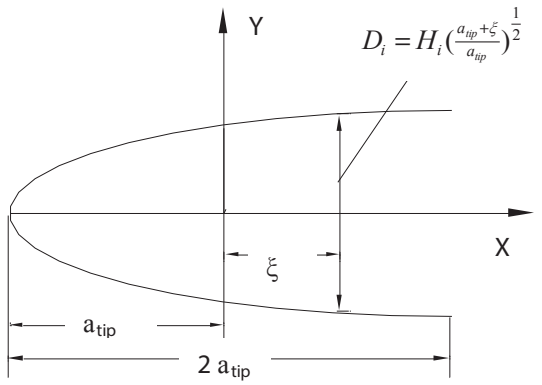

Figure 6: Schematic of the left crack tip displacement discontinuity element

For the left crack-tip displacement discontinuity element (see Fig.6), its displacement discontinuity functions are chosen as

$$D_x = H_s(\frac{a_{tip}+\xi}{a_{tip}})^{\frac{1}{2}}, \quad D_y = H_n(\frac{a_{tip}+\xi}{a_{tip}})^{\frac{1}{2}}. \tag{12}$$

where H_s and H_n are the tangential and normal displacement discontinuity quantities at the center of the element, respectively, a_{tip} is a half length of crack-tip

element. Here, it is noted that the element has the same unknowns as the two-dimensional constant displacement discontinuity element. But it can be seen that the displacement discontinuity functions defined in (12) can model the displacement fields around the crack tip. The stress field determined by the displacement discontinuity functions (12) possesses $r^{-1/2}$ singularity around the crack tip.

Based on the Eqs (10) and (11), the displacements and stresses at a point (x,y) due to the left crack-tip displacement discontinuity element can be obtained,

$$\begin{aligned} u_x &= H_s[2(1-\nu)B_3(x,y) - yB_5(x,y)] + H_n[-(1-2\nu)B_2(x,y) - yB_4(x,y)], \\ u_y &= H_s[(1-2\nu)B_2(x,y) - yB_4(x,y)] + H_n[2(1-\nu)B_3(x,y) - yB_5(x,y)], \end{aligned} \tag{13}$$

and

$$\begin{aligned} \sigma_{xx} &= 2GH_s[2B_4(x,y) + yB_6(x,y)] + 2GH_n[-B_5(x,y) + yB_7(x,y)], \\ \sigma_{yy} &= 2GH_s[-yB_6(x,y)] + 2GH_n[-B_5(x,y) - yB_7(x,y)], \\ \sigma_{xy} &= 2GH_s[-B_5(x,y) + yB_7(x,y)] + 2GH_n[-yB_6(x,y)], \end{aligned} \tag{14}$$

where functions B_2 through B_7 are described by Yan (2005b).

4.3 Implementation of the Hybrid Displacement Discontinuity Method and Some Illustrations

Crouch and Starfield (1983) used Eqs (10) and (11) to set up constant displacement discontinuity boundary element equations. Similarly, we can use Eqs (13) and (14) to set up boundary element equations associated with the crack-tip elements. The constant displacement discontinuity element together with the crack-tip elements is combined easily to form a very effective numerical approach for calculating the SIFs of general plane cracks. In the boundary element implementation, the left or the right crack-tip element is placed locally at the corresponding left or right crack tip on top of the constant displacement discontinuity elements that cover the entire crack surface and the other boundaries. The method is called a hybrid displacement discontinuity method (HDDM).

The hybrid displacement discontinuity method differs from hybrid boundary element codes by Scavia (1992) which, when used to analyze the SIFs of a branched crack, require the plate to be modeled as a finite plate of huge dimensions by fictitious stress elements, while the crack could be modeled by displacement discontinuity elements. This brings about a higher computational effort. While the hybrid displacement discontinuity method has very high accuracy and efficiency (e.g. Yan (2004c); Yan (2005c); and Yan (2006b)) .

Pan (1997) pointed out that "the displacement discontinuity method is quite suitable for cracks in infinite domain where there is no no-crack boundary. However, it

alone may not be efficient for finite domain problems, since the kernel functions in DDM involve singularities with order higher than those in the traditional displacement BEM". Recently, the hybrid displacement discontinuity method was used by Yan (2004d; 2005d and 2006c) to calculate the SIFs of complex plane cracks in a finite plate. The numerical results showed that the numerical approach was also simple, yet very accurate.

In addition, it was found from previous investigations that the hybrid displacement discontinuity method was both accurate and efficient for analyzing a multiple void-crack interaction (e.g., Yan (2006d) and Yan (2006a), a multiple cracks interaction (e.g., Yan (2003a);Yan (2005e) and Yan(2006e), a hole-crack problem(e.g.,Yan (2004a); Yan (2004b); Yan (2003b); Yan (2005a); and Yan (2006f), a mixed-mode crack problem (e.g., Yan (2006g) and Yan, Du and Zhang (1992)).

The boundary element method (BEM) also known a boundary integral equation (BIE) method has proven to be a robust and accurate numerical technique in many engineering disciplines. The attraction of BEM can be largely attributed to the reduction in the dimensionality of the problem; for 2D analysis only the line boundary of the domain needs to be discretized into elements and for 3D problems only the surface of the domain needs to be discretized. This means that, compared to domain type analysis, a boundary analysis results in a substantial reduction in data preparation and a much smaller system of equations to be solved. Furthermore, this simpler description of the body means that regions of high stress concentration can be modeled more efficiently as the necessary high concentration of grid points in confined to one less dimension. The ability of model high stress gradients accurately and efficiently has been the main reason for the method success in fracture mechanics applications (e.g., Aliabadi (1997); Dong and Atluri (2012); Dong and Atluri (2013); Cruse (1972)). Indeed, fracture mechanics has been the most active specialized area of research in the boundary element method and probably the one most exploited by industry.

Various formulations of boundary integral equation methods have been developed for elastic fracture mechanics problems. These formulations differ from each other mainly because of the different approaches used in dealing with the singularity of stress near a crack tip and the geometry identity of the surfaces of a crack. The standard boundary element formulation, when regarding the cracks as narrow slits with upper and lower surfaces slightly separated, degenerates for flat cracks and is simply not appropriate for numerical modeling (e.g, Cruse (1972)). This degeneracy is linked to the ill-posed nature of problems with two coplanar surfaces. Several different formulations have been proposed to avoid this fundamental limitation. The first one is the Green's function method by Cruse (1978), which has the advantage of avoiding crack surface modeling and gives excellent accuracy. It is however

restricted to fracture problems involving very simple crack geometries for which analytical Green's functions can be obtained. The second one is the multi-domain technique by Blandford, Ingraffea and Liggett (1981). The advantage of this approach is its ability to model cracks with any geometric shape. The disadvantage is an artificial subdivision of the original domain into several subdomains, thus resulting in a large system of equations. The third approach is the displacement discontinuity method by Crouch and Starfied (1983). Instead of using the Green's displacements and stresses from point forces, the displacement discontinuity method uses Greens functions corresponding to point dislocations (i.e., displacement discontinuity). The fourth approach is the so-called Dual Boundary Element Method (e.g., Portela, Aliabadi and Rook (1992); Mi and Aliabadi (1992); Leonel and Venturini (2010); Wang and Yao (2011)) where the displacement integral equation is collocated on the no-crack boundary and on one side of the crack surface while the traction integral equation is collocated on the other side of the crack surface. For each formulation, in order to model the singularity of stress near a crack tip, options are available such as building in the crack-tip stress singularity (e.g., Tanaka, and Itoh (1987); Kebir, Roelandt and Foulquier (1999)), using the quarter-point boundary element by Blandford, Ingraffea and Liggett (1981), and strategically refining the near-crack-tip nonsingular element. Further details on elastic crack analysis by the boundary element method are given by Aliabadi(1997) and Cruse(1989).

4.4 Computational Formulas of the Stress Intensity Factors

The objective of many analyses of linear elastic crack problems is to obtain the SIFs K_I andK_{II}. Based on the displacement field around the crack tip, the following formulas exist

$$K_I = -\frac{\sqrt{2\pi}GH_n}{4(1-\nu)\sqrt{a_{tip}}}, \qquad K_{\mathrm{II}} = -\frac{\sqrt{2\pi}GH_s}{4(1-\nu)\sqrt{a_{tip}}}. \tag{15}$$

5 Numerical Examples

To illustrate the accuracy of the numerical approach described in Section.3, numerical examples are given here.

Shown in Fig.7 are periodic collinear cracks with the same length in tension. For the crack problem, three cases, $a/d = 0.3$, $a/d = 0.5$ and $a/d = 0.95$ are analyzed by means of a generalization of Bueckner's principle and by using the Hybrid Displacement Discontinuity Method and the numerical approach described in Section 3. The calculated SIFs normalized by $\sigma\sqrt{\pi a}$ are listed in Tables 1$\sim$3. For the purpose of comparison, the corresponding exact results reported by Westergaard (1939) are also listed in these Tables.

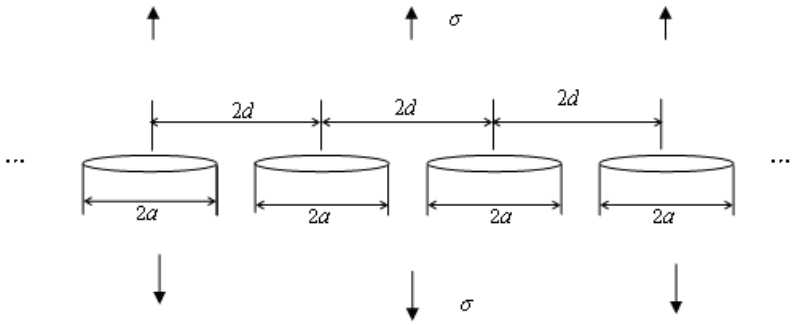

Figure 7: Schematic of periodic collinear cracks in an infinite plate in tension

In order to discuss the numerical results in Tables 1∼3, a ratio,a/d, is called a crack-distance ratio. It can be seen from Tables 1∼3 that:

(1) With an increase of the number of hole-cracks (which is equal to $2k+1$) considered in the numerical computation, the accuracy of the numerical results is increased.

(2) With an increase of the number of elements (which is N in equations (1)) considered in the numerical computation, the accuracy of the numerical results is also increased.

(3) As the crack-distance ratio, a/d, is small, in the case that the number of hole-cracks and the number of elements used in the numerical computation are not large, very accurate numerical results can be obtained. For the case of $a/d = 0.3$, for example, as the number of hole-cracks and the number of elements are 7 and 40, respectively, the calculated normalized SIF is 1.0293, while its corresponding exact one is 1.0398, whose relative error is 1%.

(4) As the crack-distance ratio, a/d, is large, as long as the number of hole-cracks and the number of elements used are large enough, very accurate numerical results can be obtained. For the case of $a/d = 0.95$, for example, as the number of hole-cracks and the number of elements are 201 and 160, respectively, the calculated normalized SIF is 2.8925, while its corresponding exact one is 2.91801, whose relative error is 0.87%.

From the numerical results in Tables 1∼3, the following experiential formula which

is used to determine the number of hole-cracks, M, can be obtained

$$M = \begin{cases} 31, & a/d \leq 0.30 \\ 51, & 0.3 < a/d \leq 0.50 \\ 71, & 0.5 < a/d \leq 0.70 \\ 101, & 0.7 < a/d \leq 0.80 \\ 141, & 0.8 < a/d \leq 0.85 \\ 161, & 0.85 < a/d \leq 0.90 \\ 181, & 0.90 < a/d \leq 0.92 \\ 201, & 0.92 < a/d \leq 0.95 \\ 251, & 0.95 < a/d \leq 0.98 \\ 301, & a/d > 0.98 \end{cases} \tag{16}$$

By means of formula (16) and the numerical approach to periodic collinear circular-hole cracks described in Section 3, periodic collinear cracks in an infinite plate in tension shown in Fig.7 are analyzed. In computations, number of elements is 100. The calculated normalized SIFs are given in Table 4 in which the exact results reported by Westergaard (1939) are also listed. From Table 4, it can be seen that the calculated normalized SIFs are in good agreement with those reported by Westergaard (1939).

Table 1: Normalized SIFs of periodic collinear cracks with the same length ($a/d = 0.3$)

Number of hole-cracks (M)	Number of elements (N)				Westergaard (1939)
	40	60	80	160	
3	1.0206	1.0216	1.0221	1.0228	
7	1.0293	1.0302	1.0307	1.0314	
11	1.0317	1.0327	1.0332	1.0339	
15	1.0329	1.0338	1.0343	1.0350	1.0398
21	1.0338	1.0348	1.0352	1.0359	
31	1.0345				
41	1.0349				
51	1.0351				
61	1.0353	1.0362	1.0367	1.0374	

Table 2: Normalized SIFs of periodic collinear cracks with the same length ($a/d = 0.5$)

Number of hole-cracks (M)	Number of elements (N)				Westergaard (1939)
	40	60	80	160	
3	1.0744	1.0756	1.0761	1.0769	
7	1.1018	1.1030	1.1036	1.1045	
11	1.1096	1.1109	1.1115	1.1124	1.1284
15	1.1134	1.1146	1.1152	1.1161	
21	1.1163	1.1175	1.1181	1.1190	
61	1.1212	1.1224	1.1230	1.1238	

Table 3: Normalized SIFs of periodic collinear cracks with the same length ($a/d = 0.95$)

Number of hole-cracks (M)	Number of elements (N)			Westergaard (1939)
	80	160	320	
11	2.6300	2.6465	2.6550	
21	2.7415	2.7592	2.7678	
31	2.7833	2.8014	2.8097	
41	2.8052	2.8232	2.8318	
51	2.8187	2.8365	2.8453	2.91801
61	2.8278	2.8456	2.8544	
71	2.8342	2.8521	2.8610	
91	2.8428	2.8609	2.8699	
101	2.8458	2.8640	2.8730	
151		2.8782		
201		2.8925		

Table 4: Normalized SIFs of periodic collinear cracks with the same length

a/d	0.05	0.10	0.20	0.30	0.40	0.50	0.60	0.70	0.80	0.90
SIFs	0.9991	1.0021	1.0144	1.0362	1.0713	1.1228	1.2019	1.3262	1.5517	2.0926
Westergaard (1939)		1.0041	1.0170	1.0398	1.0753	1.1284	1.2085	1.3360	1.5650	2.1133

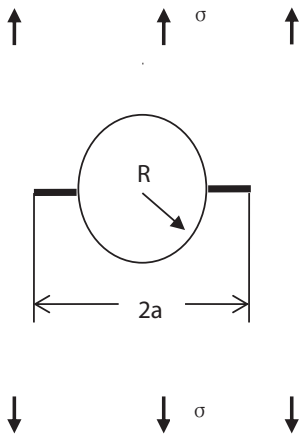

Figure 8: A circular-hole crack in an infinite plate in tension

6 Numerical Results and Discussions

Before analyzing periodic collinear circular-hole cracks in an infinite plate in tension shown in Fig.1, in this section, first a circular-hole crack in an infinite plate in tension shown in Fig.8 is analyzed by means of a generalization of Bueckner's principle and by using the Hybrid Displacement Discontinuity Method. The calculated SIFs can be expressed mathematically as $K_{Ich}(a/R)$. If the SIFs of the center crack of the length $2a$ are expressed as K_{Icc}, then their ratio denoted by F_{Ich} is,

$$F_{Ich} = K_{Ich}(a/R)/K_{Icc} = K_{Ich}(a/R)/(\sigma\sqrt{\pi a}). \tag{17}$$

which is called a normalized SIFs. The calculated normalized SIFs F_{Ich} are given in Table 5, also see Fig.9. For the purpose of comparison, Table 6 lists the numerical results reported by Bowie (1956). From Tables 5 and 6 it can be seen that the calculated SIFs are in excellent agreement with those reported by Bowie (1956).

From Fig.9 it is found that:

(a) With an increase of $a_r(= a/R)$, F_{Ich} fast increases monotonously. At a certain value a_{rc}, $F_{Ich} = 1$, i.e., K_{Ich} equals K_{Icc}. Here, $a_{rc} = 1.23$.

(b) With continuous increase of a_r, F_{Ich} begins to increase slowly and reaches its maximum F_{Ichm} at some value a_{rm}. Here, $a_{rm} = 1.50$, $F_{Ichm} = 1.0572$.

(c) Continuous increase of a_r leads to F_{Ich} to begin to decrease slowly and F_{Ich} is almost equal to 1 (i.e., K_{Ich} is almost equal to K_{Icc}) when a_r is large enough (e.g., greater than a_{rcl}). Here, $a_{rcl} = 5.0$.

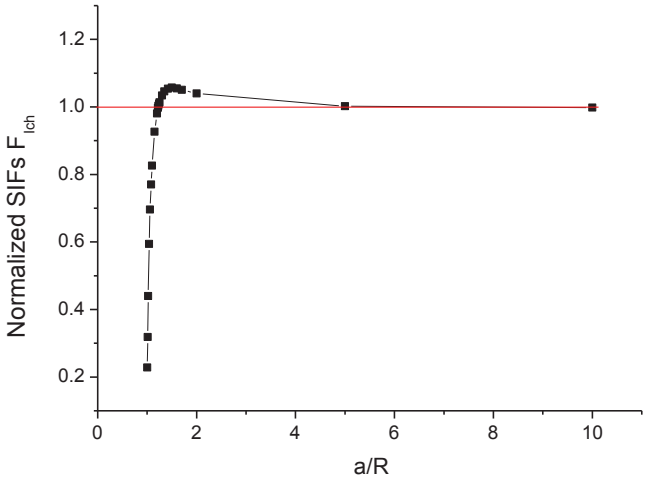

Figure 9: Normalized SIFs of a circular hole crack in an infinite plate in tension

After introducing the dimensionless parameters a_{rc}, a_{rm}, a_{rcl} and F_{Ichm}, it is found that:

(1) As $a_r < a_{rc}$, a circular hole has a **shielding effect** on the cracks emanating from the circular hole. And the closer the size of the circular hole is to that of the crack, the stronger the shielding effect is.

(2) As $a_r > a_{rc}$, the circular hole has an **amplifying effect** on the SIFs of the center crack and the amplifying effect is the most obvious at $a_r = a_{rm}$.

(3) As a_r is large enough (greater than a_{rcl}), i.e., the size of the circular hole is small enough relative to that of the center crack, the effect of the circular hole on the SIFs of the center crack is almost neglected.

Table 5: Normalized SIFs of a circular hole crack in an infinite plate in tension

a/R	1.005	1.01	1.02	1.04	1.06	1.08	1.10	1.15	1.20	1.22	1.23
SIFs	0.2279	0.3183	0.4400	0.5939	0.6957	0.7699	0.8264	0.9264	0.9807	0.9971	1.0035
a/R	1.24	1.25	1.30	1.35	1.42	1.50	1.60	1.70	2.00	5.00	10.0
SIFs	1.0094	1.0136	1.0339	1.0456	1.0540	1.0572	1.0547	1.0504	1.0395	1.0021	0.9981

Periodic collinear circular-hole cracks in an infinite plate in tension are analyzed in detail by means of a generalization of Bueckner's principle and by using the Hybrid Displacement Discontinuity Method, the numerical approach to periodic collinear

Table 6: Normalized SIFs of a circular hole crack in an infinite plate in tension [Bowie (1956)]

a/R	1.02	1.04	1.06	1.08	1.10	1.15	1.25	1.50	2.50	4.0
SIFs	0.4514	0.6082	0.7104	0.7843	0.8400	0.9322	1.0168	1.0582	1.0252	1.0077

circular-holes cracks described in Section 3 and formula (17). The following cases are considered:

$a/d = 0.05, 0.20, 0.40, 0.70, 0.80, 0.84, 0.88, 0.90$
$a/R = 1.02, 1.04, 1.06, 1.08, 1.10, 1.15, 1.25, 1.50, 2.50, 4.0$

Regarding discretizations, the number of elements on a branched crack is given in Table 7, the other boundaries are discretized according to such a limitation that all boundary elements have approximately the same length.

If the calculated SIFs normalized by $\sigma\sqrt{\pi a}$ are denoted by F_{Ipccc}, obviously, F_{Ipccc} can be expressed mathematically as

$$F_{Ipccc} = F_{Ipccc}(a/R, a/d) \tag{18}$$

If we let the SIFs normalized by $\sigma\sqrt{\pi a}$ for periodic collinear cracks with same length in an infinite plate in tension (see Fig.7) be denoted by F_{Ipcc} then F_{Ipcc} can be expressed mathematically as

$$F_{Ipcc} = F_{Ipcc}(a/d) \tag{19}$$

The calculated normalized SIFs F_{Ipccc} are given in Table 8. The normalized SIFs F_{Ipcc} are listed in Table 4. It can be seen from Tables 8 and 5 and 4 that:

(1) When a/d is very small, for example, $a/d = 0.05$, the interactions of periodic collinear circular-hole cracks can be neglected. At this time, the normalized SIFs $F_{Ipccc}$are almost equal to those of a circular-hole crack F_{Ich}.

(2) When a/R is large enough, for example, $a/R = 4.00$, the effect of circular holes on the SIFs can be neglected. At this time, the normalized SIFs F_{Ipccc} are almost equal to those corresponding to periodic collinear cracks with the same crack length and the same spacing.

The above two points illustrate that the numerical results obtained for periodic collinear circular-hole cracks in an infinite plate in tension are accurate and effective.

From Table 8, it can be seen that, for any a/R, variations of the normalized SIFs F_{Ipccc} of periodic collinear circular-hole cracks with a/d are similar to those of the

normalized SIFs F_{Ipcc} of periodic collinear cracks. For $a/R = 1.04, 1.10, 4.00$, for example, the SIFs F_{Ipccc} are shown in Fig.10, from which the observation can be proven.

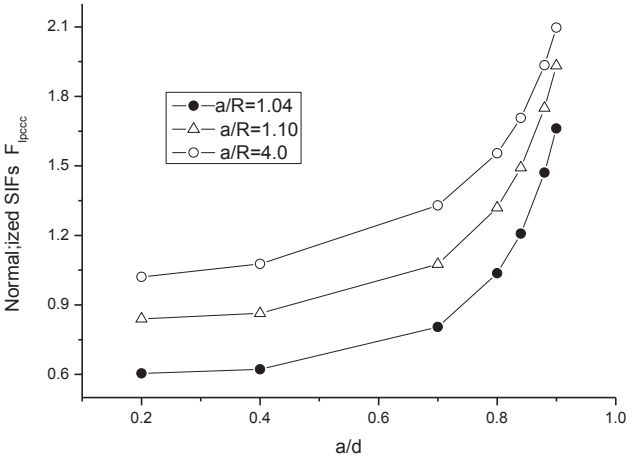

Figure 10: Normalized SIFs for periodic collinear circular-hole cracks in an infinite plate in tension

From Table 8, it can be also seen that, for any a/d, variations of the normalized SIFs F_{Ipccc} of periodic collinear circular-hole cracks with a/R are similar to those of the normalized SIFs F_{Ich} of a circular hole crack. For $a/d = 0.05, 0.70, 0.90$, for example, the SIFs F_{Ipccc} are shown in Fig.11, from which the observation can be proven.

Based on discussions on an effect of a circular hole on a crack emanating from the circular hole in an infinite plate in tension and the similarity of variations of the SIFs $F_{Ipccc}(a/R, a/d)$ with a/R to that of the SIFs $F_{Ich}(a/R)$ with a/R, we come to conclude that there are also shielding and amplifying effects for periodic collinear circular-hole cracks in an infinite plate in tension. The shielding and amplifying effects perhaps have an important meaning in engineering. For example, suppose that there are periodic collinear cracks in an infinite plate in tension with $a/d = 0.80$. From Table 4, the normalized SIF is 1.5650. Here, suppose also that periodic circular holes are cut out on the periodic collinear cracks with $a/R = 1.04$. From Table 8, the normalized SIF is 1.0367. Thus it can be concluded from these data that the plate with the periodic collinear circular-hole cracks with $a/R = 1.04$ is much safer than that with the periodic collinear cracks.

Table 7: Variations of element number on a branch crack with a/R

a/R	1.02	1.04	1.06	1.08	1.10	1.15	1.25	1.50	2.50	4.0
Element Number	7	14	18	20	25	30	50	80	150	450

Table 8: Normalized SIFs for periodic collinear circular-hole cracks in an infinite plate in tension

a/d	a/R									
	1.02	1.04	1.06	1.08	1.10	1.15	1.25	1.50	2.50	4.0
0.05	0.4435	0.6029	0.7061	0.7807	0.8373	0.9302	1.0159	1.0581	1.0249	1.0063
0.20	0.4445	0.6045	0.7082	0.7832	0.8402	0.9341	1.0216	1.0672	1.0389	1.0212
0.40	0.4571	0.6215	0.7280	0.8051	0.8636	0.9606	1.0527	1.1070	1.0917	1.0770
0.70	0.6036	0.8049	0.9280	1.0135	1.0760	1.1765	1.2699	1.3315	1.3374	1.3292
0.80	0.7986	1.0367	1.1707	1.2585	1.3194	1.4132	1.4963	1.5513	1.5603	1.5540
0.84	0.9475	1.2080	1.3465	1.4337	1.4923	1.5799	1.6548	1.7037	1.7127	1.7069
0.88	1.1837	1.4709	1.6117	1.6961	1.7501	1.8281	1.8915	1.9318	1.9396	1.9342
0.90	1.3639	1.6613	1.8013	1.8825	1.9332	2.0081	2.0609	2.0958	2.1026	2.0973

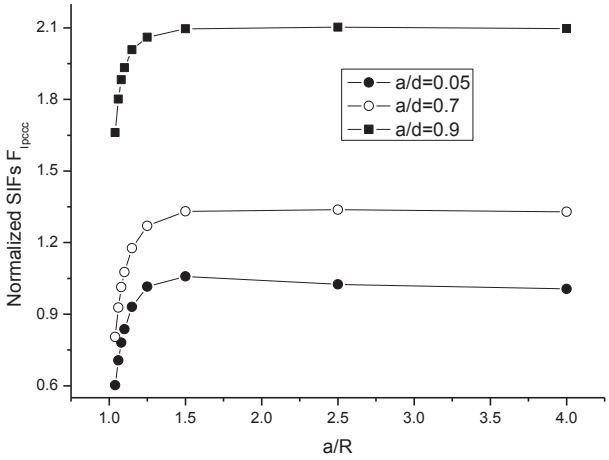

Figure 11: Normalized SIFs for periodic collinear circular-hole cracks in an infinite plate in tension

7 Conclusions

Based on the present investigations, the following conclusions can be made:

1. A numerical approach to periodic collinear circular-hole cracks is presented. Numerical examples are included to illustrate the accuracy of the numerical approach.

2. Periodic collinear circular-hole cracks in an infinite plate in tension are investigated in detail by using the numerical approach. Many numerical results of the SIFs are given and discussed. It is found that there are also shielding and amplifying effects for periodic collinear circular-hole cracks in an infinite plate in tension. The shielding and amplifying effects perhaps have an important meaning in engineering.

Acknowledgement

Special thanks are due to the National Natural Science Foundation of China (No.10272037 and No.10672046) for supporting the present work.

References

Aliabadi, M. H. (1997): Boundary element formulation in fracture mechanics. *Applied Mechanics Review*, vol. 50, pp. 83-96.

Blandford, G. E.; Ingraffea, A. R.; Liggett, J. A. (1981): Two-Dimensional Stress Intensity Factor Computations Using the Boundary Element Method. *Int J. Num Methods Eng.*, vol. 17, pp. 387-404.

Bleuth, J. L.; Hutchinson, J. W. (1994): Fracture analysis of multi-site cracking in fuselage lap joints. *Comput. Mech.,* vol. 13, pp. 315–331.

Bowie, O. L. (1956): Analysis of an infinite plate containing radial cracks originating at the boundary of an internal circular hole. textitJ. Math. Phys., vol. XXXV, no. 1, pp. 60-71.

Buckner, H. F. (1959): The propagation of cracks and the energy of elastic deformation. ASME *J. Appl. Mech*., vol. 80, pp. 1225-1230.

Cai, H. T.; Lu, J. K. (2009): First fundamental problems of anisotropic elastic plane weakened by periodic collinear cracks. *Applied Mathematics and Mechanics,* vol. 30, no. 3, pp. 1429-1436.

Chen, Y. Z. (2011): Solutions of periodic notch problems with arbitrary configuration by using boundary integral equation and superposition method. *ACTA Mechanica*, vol. 221, no. 3-4, pp. 251-260.

Chen, Y. Z.; Lin, X. Y. (2007): Solution of periodic group circular hole problems by using the series expansion variational method. *Int. J. Numer. Meth. Engng,* vol. 69, pp. 1405–1422.

Crouch, S. L.; Starfied, A. M. (1983): *Boundary Element Method in Solid Mechanics*. London, Geore Allon & Unwin, Bonton, Sydney.

Cruse, T. A. (1972): *Numerical Evaluation of Elastic Stress Intensity Factors by Boundary Integral Equation Method, in "Surface Cracks Physics Problems and Computational Solutions"*. Swedlow J.L. (ed), ASME, New York, pp. 153-170.

Cruse, T. A. (1978): Two-dimensional BIE fracture mechanics analysis. *Appl. Math. Modelling*, vol. 2, pp. 287-293.

Cruse, T. A. (1989): Boundary Element Analysis in Computational Fracture Mechanics, Dordrecht: Kluwer, pp. 1-230.

Dong, L.; Atluri, S. N. (2012): SGBEM(Using Non-hyper-singular Traction BIE), and Super Elements, for Non-Collinear Fatigue-growth Analyses of Cracks in Stiffened Panels with Composite-Patch Repairs. *Computer Modeling in Engineering & Sciences*, vol. 89, no. 5, pp. 415-456.

Dong, L.; Atluri, S. N. (2013): Fracture & Fatigue Analyses: SGBEM-FEM or XFEM? Part 1: 2D Structures. *CMES: Computer Modeling in Engineering & Sciences,* vol. 90, no. 2, pp. 91-146.

Hausler, C.; Gao, C. F.; Balke, H. (2004): Collinear and periodic electrode-ceramic interfacial cracks in piezoelectric bimaterials. *Trans. ASME, Journal of Applied Mechanics,* vol. 71, no. 4, pp. 486-492.

Horii, H.; Nemat-Nasser, S. (1985): Elastic fields of interacting in homogeneities. *International Journal of Solids and Structure,* vol. 21, pp. 731–745.

Hu, Y. T.; Huang, Y. Y.; Cheng, L. Z. (1998): Periodic elliptic holes in anisotropic elasticity. *Mechanics Research Communications,* vol. 25, no. 2, pp. 171-178.

Hu, Y. T.; Huang, Y. Y.; Zhong, W. F. (1997): Collinear periodic cracks in anisotropic bimaterials. *International Journal of Fracture,* vol. 85, no. 1, pp. 69-80.

Hu, Y. T.; Zhao, X. H. (1996): Collinear periodic cracks in an anisotropic medium. *International Journal of Fracture,* vol. 76, no. 3, pp. 207-219.

Iovane, G.; Sumbatyan, M. A. (2009): Periodic system of collinear cracks in an elastic porous medium. *Mechanics of Solids,* vol. 44, no. 3, pp. 400-408.

Irwin, G. R. (1957): Analysis of stresses and strains near the end of a crack transvering a plate. *Trans.ASME, Journal of Applied Mechanics,* vol. 24, pp. 361.

Kebir, H.; Roelandt, J. M.; Foulquier, J. (1999): A new singular boundary ele-

ment for crack problems. *Application to bolted joints. Engineering Fracture Mechanics,* vol. 69, pp. 497-510.

Koiter, W. T. (1959): An infiniter row of collinear cracks in an infinite elastic sheet. *Ingenieur-Archiv,* vol. 28, pp. 168-177.

Lekesiz, H.; Katsube, N.; Rokhlin, S. I. (2011): Effective spring stiffness for a planar periodic array of collinear cracks at an interface between two dissimilar isotropic materials. *Mechanics of Materials,* vol. 43, no. 2, pp. 87-98.

Leonel, E. D.; Venturini, W. S. (2010): Boundary element formulation applied to analysis of multi-fractured domains. *Engineering Analysis with Boundary Elements,* vol. 34, pp. 1092-1099.

Mi, Y.; Aliabadi, M. H. (1992): Dual- boundary element method for three dimensional fracture mechanics analysis. *Eng. Ana. with Boundary Elements,* vol. 10, pp. 161-171.

Nemet-Nasser, S.; Yu, N.; Horii, M. (1993): Solids with periodically distributed cracks. *International Journal of Solids Structure,* vol. 30, pp. 2071–2095.

Ouinas, D. (2012): Strength of aluminum single-lap bonded joints in various disbond size at circular and semi-circular notches. *Journal of Sandwich Structures & Materials,* vol. 14, no. 6, pp. 753-768.

Pan, E. (1997): A General Boundary Element Analysis of 2-D Linear Elastic Fracture Mechanics. *Int J Fract,* vol. 88, pp. 41-59.

Portela, A.; Aliabadi, M. H.; Rook, D. P. (1992): The dual boundary element method: effective implementation for crack problems. *Int. J. Num. Methods Eng.*, vol. 33, pp. 1269-1287.

Scavia, C. (1992): A numerical technique for the analysis of cracks subjected to normal compressive stresses. *Int J Num Methods Eng.,* vol. 33, pp. 929-942.

Tanaka, M.; Itoh, H. (1987): New crack elements for boundary element analysis of elastostatics considering arbitrary stress singularities. *Appl Math Modelling,* vol. 11, pp. 357-363.

Wang, G. S.; Feng, X. T. (2001): The interaction of multiple rows of periodical cracks. *International Journal of Fracture,* vol. 110, pp. 73–100.

Wang, H. T.; Yao, Z. H. (2011): A fast multiple dual boundary element method for the three-dimensional crack problems. *Computer Modeling in Engineering & Sciences,* vol. 72, no. 2, pp. 115-147.

Westergaard, H. M. (1939): Bearing Pressures and Cracks. *Trans. ASME, J. Appl. Mech.*, vol. 6, no. 2, pp. 49-53.

Yan, X. (2003a): Analysis of the interference effect of arbitrary multiple parabolic

cracks in plane elasticity by using a new boundary element method. *Computer Methods in Applied Mechanics and Engineering,* vol. 192, no. 47-48, pp. 5099-5121.

Yan, X. (2003b): An effective method of stress intensity factor calculation for cracks emanating form a triangular or square hole under biaxial loads. *Fatigue and Fracture of Engineering Materials and Structures*, vol. 26, no. 12, pp. 1127-1133.

Yan, X. (2004a): Interaction of arbitrary multiple cracks in an infinite plate. *J Strain Analysis for Engineering Design*, vol. 39, no. 3, pp. 237-244.

Yan, X. (2004b): Analysis for a crack emanating form a corner of a square hole in an infinite plate using the hybrid displacement discontinuity method. *Appl Math Modeling,* vol. 28, no. 9, pp. 835-847.

Yan, X. (2004c): A numerical analysis of perpendicular cracks under general in-plane loading with a hybrid displacement discontinuity method. *Mechanical Research Communications*, vol. 31, no. 2, pp. 175-183.

Yan, X. (2004d): A numerical analysis of cracks emanating from a square hole in a rectangular plate under biaxial loads. *Eng Fracture Mech.*, vol. 71, no. 11, pp. 1615-1623.

Yan, X. (2005a): Stress intensity factors for cracks emanating form a triangular or square hole in an infinite plate by boundary elements. *Engineering Failure Analysis,* vol. 12, no. 3, pp. 362-375.

Yan, X. (2005b): An efficient and accurate numerical method of SIFs calculation of a branched crack. *ASME J. Appl. Mech.*, vol. 72, no. 3, pp. 330-340.

Yan, X. (2005c): Stress intensity factors for asymmetric branched cracks in plane extension by using crack tip displacement discontinuity elements. *Mechanics Research Communications,* vol. 32, no. 4, pp. 375-384.

Yan, X. (2005d): An effective boundary element method for analysis of crack problems in a plane elastic plate. *Appl Math Mech,* vol. 26, no. 6, pp. 814-822.

Yan, X. (2005e): Microdefect interacting with a finite main crack. *J Strain Analysis for Engineering Design*, vol. 40, no. 5, pp. 421-430.

Yan, X. (2006a): An effective numerical approach for multiple void-crack interaction. *ASME J. Appl. Mech.*, vol. 73, no. 4, pp. 525-535.

Yan, X. (2006b): A numerical analysis of stress intensity factors at bifurcated cracks. *Engineering Failure Analysis,* vol. 13, no. 4, pp. 629-637.

Yan, X. (2006c): A numerical analysis of cracks emanating from an elliptical hole in a 2-D elasticity plate. *European J of Mechanics-A*, vol. 25, no. 1, pp. 142-153.

Yan, X. (2006d): A finite main crack interaction with an arbitrarily oriented mi-

crodefect. *Engineering Failure Analysis,* vol. 13, pp. 971–980.

Yan, X. (2006e): A brief evaluation of approximation methods for microcrack shielding problems. *ASME J. Appl. Mech.,* vol. 73, no. 4, pp. 694-696.

Yan, X. (2006f): Cracks Emanating from Circular Hole or Square Hole in Rectangular Plate in Tension. *Eng Fracture Mech.*, vol. 73, no. 12, pp. 1743-1754.

Yan, X. (2006g): Numerical analysis of stress intensity factor for two kinds of mixed-mode crack specimens. *J Strain Analysis for Engineering Design,* vol. 41, no. 1, pp. 9-18.

Yan, X.; Du, S.; Zhang, Z. (1992): Mixed-mode fatigue crack growth prediction in biaxially stretched sheets. *Eng. Fract. Mech.,* vol. 43, pp. 471-475.